

**JAERI-Research**  
**94-008**



**THERMAL DURABILITY OF MODIFIED SYNROC MATERIAL  
AS REACTOR FUEL MATRIX**

**August 1994**

**Akira KIKUCHI, Hiroyuki KANAZAWA, Yoshihiro TOGASHI  
Seiichiro MATUMOTO, Yasuharu NISHINO, Isao OHWADA  
Masahito NAKATA, Hidetoshi AMANO and Hisayoshi MITAMURA**

**日本原子力研究所**  
**Japan Atomic Energy Research Institute**

本レポートは、日本原子力研究所が不定期に公刊している研究報告書です。

入手の問合わせは、日本原子力研究所技術情報部情報資料課（〒319-11 茨城県那珂郡東海村）あて、お申し越してください。なお、このほかに財団法人原子力弘済会資料センター（〒319-11 茨城県那珂郡東海村日本原子力研究所内）で複写による実費領布をおこなっております。

This report is issued irregularly.

Inquiries about availability of the reports should be addressed to Information Division, Department of Technical Information, Japan Atomic Energy Research Institute, Tokai-mura, Naka-gun, Ibaraki-ken 319-11, Japan.

© Japan Atomic Energy Research Institute, 1994

---

編集兼発行 日本原子力研究所  
印刷 ㈱原子力資料サービス

Thermal Durability of Modified Synroc Material as Reactor Fuel Matrix

Akira KIKUCHI, Hiroyuki KANAZAWA, Yoshihiro TOGASHI  
Seiichiro MATUMOTO, Yasuharu NISHINO, Isao OHWADA  
Masahito NAKATA, Hidetoshi AMANO and Hisayoshi MITAMURA<sup>+</sup>

Department of Hot Laboratories  
Tokai Research Establishment  
Japan Atomic Energy Research Institute  
Tokai-mura, Naka-gun, Ibaraki-ken

(Received July 1, 1994)

A Synroc, a polyphase titanate ceramics composed of three mineral phases (perovskite, hollandite and zirconolite), has an excellent performance of immobilization of high level nuclear waste. A working group in the Department of Hot Laboratories paid special attention to this merit and started a development study on a LWR fuel named "Waste Disposal Possible (WDP) Fuel", which has the two functions of a reactor fuel and a waste form. The present paper mainly describes thermal durability of a modified Synroc material, which is essentially important for applying the material to a fuel matrix.

The two kinds of Synroc specimens, designated "SM" as modified and "SB" as a reference, were prepared by hot-pressing and annealed at 1200 °C to 1500 °C for 30 min in air. Unexpected and peculiar spherical voids were observed in the specimen SM at 1400 °C and 1500 °C, which caused the specimen swelling. The formation of the voids depends significantly on the existence of spherical precipitates seen in the as-fabricated specimen including latent micropores with high pressure. On the other hand, the heat treatment at 1500 °C formed additional new phases, designated "Phase A" for the specimen SB and "Phase X" for SM. Phase A is a decomposition product of hollandite and Phase X a reaction product of Phase A and perovskite in the spherical voids.

Furthermore, additional information and thermal properties examined are presented in Appendix 1 and Appendix 2, respectively. It was recognized that the

---

<sup>+</sup>Department of Environmental Safety Research

modified Synroc specimen SM had excellent thermal properties.

Keywords: Waste Disposal Possible Fuel, Modified Synroc Material, Thermal Durability, Spherical Void, Thermal Diffusivity Measurement, Melting Experiment

## 原子炉用燃料マトリックスとしての改良シンロック材の熱的耐久性

日本原子力研究所東海研究所ホット試験室

菊地 章・金沢 浩之・富樫 喜博・松本征一郎

西野 泰治・大和田 功・仲田 祐仁・天野 英俊

三田村久吉<sup>+</sup>

(1994年7月1日受理)

シンロックはペロブスカイト、ホランダイト及びジルコノライトから成るチタン酸セラミックスで、高レベル放射性廃棄物の閉じ込めに優れた性能を有している。ホット試験室のワーキンググループでは、この点に着目し、“廃棄処理可能(WDP)燃料”の開発研究に着手した。これは、燃料としての機能を有するとともに、固化体としての機能を同時に有するものである。手始めとして、改良シンロック材の熱的耐久性を求めた。これは、燃料マトリックスとしての応用において、本質的に重要なものである。

2種のシンロック試料、すなわち改良シンロック SM 及び参照シンロック SB、を作製し、1200 度Cから1500 度Cで30 分間、空気中での熱処理を行った。試料 SM では、1500 度C及び1400 度Cの熱処理で試料に膨れを及ぼす予期せぬ球状ボイドを見た。このボイドは、作製した試料に生じていた球状析出物とそれが含む潜在高圧微小ボアーの存在に大きく依存している。一方、1500 度Cの熱処理では、試料 SB において新相A相が、また試料 SM ではX相が生成した。A相はホランダイトの分解、またX相はこのA相とペロフスカイトの反応によるものである。

なお、本報に関連して、付加的情報及び熱的性質についての実験とその結果とを付録1及び2に述べる。実験では、改良シンロック材の熱的性質の優れていることが認められた。

## Contents

1. Introduction .....	1
2. Experimental Methods .....	1
2.1 Specimen .....	1
2.2 Heat Treatment .....	2
2.3 Measurement .....	2
3. Results .....	2
3.1 Deformation .....	2
3.2 Microstructure .....	2
3.3 Phase .....	3
3.4 Others .....	3
4. Discussion .....	3
4.1 Growth Mechanism of Spherical Void .....	3
4.2 Formation Mechanism of New Phases .....	4
5. Conclusion .....	5
Acknowledgement .....	6
References .....	6
Appendix Additional Information and Thermal Properties .....	6

## 目 次

1. 序 論 .....	1
2. 実 験 法 .....	1
2.1 試 料 .....	1
2.2 熱 処 理 .....	2
2.3 測 定 .....	2
3. 結 果 .....	2
3.1 変 形 .....	2
3.2 微細組織 .....	2
3.3 相 .....	3
3.4 その他 .....	3
4. 検 討 .....	3
4.1 球状ボイドの成長機構 .....	3
4.2 新相の生成機構 .....	4
5. 結 論 .....	5
謝 辞 .....	6
参考文献 .....	6
付 録 付加的情報及び熱的性質 .....	6

## 1. Introduction

A polyphase titanate ceramic named Synroc (Synthetic Rock) has been developed for the immobilization of high level nuclear waste (HLW)<sup>1), 2)</sup>. This material has an excellent confinement performance for FPs and TRUs in HLW (see Appendix 1). For this reason, the Synroc material was taken up as a matrix of a reactor fuel, because the fuel matrix itself would act as a waste form during burnup. Using the Synroc material of which the phase composition was slightly modified, we started a development study on a matrix of the fuel named "Waste Disposal Possible (WDP) Fuel" for a LWR, which has the two functions of the reactor fuel and the waste form.

Synroc consists mainly of three mineral phases<sup>3), 4)</sup>: perovskite ( $\text{CaTiO}_3$ ), hollandite ( $\text{BaAl}_2\text{Ti}_6\text{O}_{16}$ ) and zirconolite ( $\text{CaZrTi}_2\text{O}_7$ ). Since the latter two phases have relatively lower melting points around  $1500^\circ\text{C}$  (see Appendix 1), the Synroc material is intuitively not considered to be suitable for the reactor fuel matrix. At present, however, there are few data on thermal durability (and thermal properties) of the Synroc material at high temperature<sup>5), 6)</sup>. This makes it difficult to decide its use for the fuel matrix. From this standing points, our emphasis was placed on the investigation of thermal behavior of the modified Synroc material at high temperature.

In the present study, the two kinds of Synroc specimens, designated "SM" and "SB", were prepared and heat treated for getting data about changes in their shapes, microstructures, phase compositions, etc. The heat treatment was principally carried out at  $1500^\circ\text{C}$  which was close to the melting temperature of hollandite phase. Other heat treatment at  $1200^\circ\text{C}$  to  $1400^\circ\text{C}$  were also conducted to examine unexpected phenomena in the heat treatment at  $1500^\circ\text{C}$ . Furthermore, additional experiments and results on thermal properties at high temperature are summarized in Appendix 2.

## 2. Experimental Methods

### 2.1 Specimen

The two kinds of Synroc specimens were prepared (Table 1): one is a modified Synroc material, designated "SM", as a principal specimen in the present study, and the other a Synroc B material, designated "SB", as a reference specimen. The specimen SM includes 60 % of perovskite and no rutile. The phase composition of this specimen was chosen to improve the thermal durability of the specimen SB. The amount of zirconolite was decided on the basis of the least loading content of plutonium in future.

The preparation process of the specimens is shown in Fig. 1. The precursors were prepared through hydrolysis of alkoxide reagents and calcined at around  $750^\circ\text{C}$  for 2 hr in a stream of Ar-4% $\text{H}_2$  gas. The calcined products were hot-pressed using a graphite die at  $1200^\circ\text{C}$  and 29 MPa for 2 hr in a stream of  $\text{N}_2$  gas. As-cast specimen cylinders were about 20 mm in diameter and about 10 mm in length. The outside views of these specimens are shown in Fig. 2, and macrostructure in a cross section of the specimen SM is indicated in Fig. 3. The specimen SM shows a heterogeneous feature in its macrostructure, while the specimen SB had a



## 1. Introduction

A polyphase titanate ceramic named Synroc (Synthetic Rock) has been developed for the immobilization of high level nuclear waste (HLW)<sup>1), 2)</sup>. This material has an excellent confinement performance for FPs and TRUs in HLW (see Appendix 1). For this reason, the Synroc material was taken up as a matrix of a reactor fuel, because the fuel matrix itself would act as a waste form during burnup. Using the Synroc material of which the phase composition was slightly modified, we started a development study on a matrix of the fuel named "Waste Disposal Possible (WDP) Fuel" for a LWR, which has the two functions of the reactor fuel and the waste form.

Synroc consists mainly of three mineral phases<sup>3), 4)</sup>: perovskite ( $\text{CaTiO}_3$ ), hollandite ( $\text{BaAl}_2\text{Ti}_6\text{O}_{16}$ ) and zirconolite ( $\text{CaZrTi}_2\text{O}_7$ ). Since the latter two phases have relatively lower melting points around  $1500^\circ\text{C}$  (see Appendix 1), the Synroc material is intuitively not considered to be suitable for the reactor fuel matrix. At present, however, there are few data on thermal durability (and thermal properties) of the Synroc material at high temperature<sup>5), 6)</sup>. This makes it difficult to decide its use for the fuel matrix. From this standing points, our emphasis was placed on the investigation of thermal behavior of the modified Synroc material at high temperature.

In the present study, the two kinds of Synroc specimens, designated "SM" and "SB", were prepared and heat treated for getting data about changes in their shapes, microstructures, phase compositions, etc. The heat treatment was principally carried out at  $1500^\circ\text{C}$  which was close to the melting temperature of hollandite phase. Other heat treatment at  $1200^\circ\text{C}$  to  $1400^\circ\text{C}$  were also conducted to examine unexpected phenomena in the heat treatment at  $1500^\circ\text{C}$ . Furthermore, additional experiments and results on thermal properties at high temperature are summarized in Appendix 2.

## 2. Experimental Methods

### 2.1 Specimen

The two kinds of Synroc specimens were prepared (Table 1): one is a modified Synroc material, designated "SM", as a principal specimen in the present study, and the other a Synroc B material, designated "SB", as a reference specimen. The specimen SM includes 60 % of perovskite and no rutile. The phase composition of this specimen was chosen to improve the thermal durability of the specimen SB. The amount of zirconolite was decided on the basis of the least loading content of plutonium in future.

The preparation process of the specimens is shown in Fig. 1. The precursors were prepared through hydrolysis of alkoxide reagents and calcined at around  $750^\circ\text{C}$  for 2 hr in a stream of Ar-4% $\text{H}_2$  gas. The calcined products were hot-pressed using a graphite die at  $1200^\circ\text{C}$  and 29 MPa for 2 hr in a stream of  $\text{N}_2$  gas. As-cast specimen cylinders were about 20 mm in diameter and about 10 mm in length. The outside views of these specimens are shown in Fig. 2, and macrostructure in a cross section of the specimen SM is indicated in Fig. 3. The specimen SM shows a heterogeneous feature in its macrostructure, while the specimen SB had a

homogeneous macrostructure. In the figure, black spots in the specimen SM are not voids, but spherical precipitates. Electron probe microanalysis (EPMA) revealed that the spherical precipitates were rich in calcium and poor in titanium. This implies that these precipitates include higher content of perovskite than the matrix, because X-ray diffractometry (Fig. 4) does not indicate the formation of any other additional phase in the as-fabricated specimen SM.

## 2.2 Heat Treatment

Sector specimens of about 1.5 gm were annealed on an alumina dish at 1200 °C to 1500 °C for 30 min in air. The last maximum temperature is nearly equal to the melting point of the hollandite phase.

## 2.3 Measurement

The density of the specimen was measured by the water displacement method. The swelling rate of the specimen was calculated from its density change after heat treatment. The average grain size of perovskite crystals and the characteristics of spherical voids mentioned latter were analyzed by image processing after capture of secondary electron images (SEI) and backscattered electron images (BSI).

## 3. Results

### 3.1 Deformation

The outside views of the specimen SM after the heat treatments at 1500 °C and 1400 °C are shown in Fig. 5. The outer zone of the specimen is partly deformed after heating at 1500 °C, although the specimen retains its shape at 1400 °C. On the other side, the specimen SB entirely got out of shape at 1500 °C. These phenomena might be caused by the melting of hollandite crystals, and softening of hollandite and zirconolite crystals. The summary of data from the specimen SM is presented in Table 2. In the table, the specimen SM shows the swelling rates of about 18 and 25 % at 1500 °C and 1400 °C, respectively. The reason why the rate was larger at the lower temperature is supposed to be due to a thermal stability in microstructures as described in the following section. No remarkable swelling occurred in the specimen below 1300 °C.

### 3.2 Microstructure

A peculiar microstructure was observed in the specimen SM after the heat treatment at 1500 °C. As shown in the microstructure in Fig. 6, fine spherical voids are distributed in the specimen matrix. In the figure, the right-edge zone is of the deformed part named "Falling-down zone (F)". Enlarged images of the voids are indicated in Fig. 7. The feature of the void is divided into the two types, A and B : The type-A void is filled with the separated polyhedral crystals of perovskite, while the type-B void is covered with a film. EPMA reveals that the film was composed of hollandite and zirconolite. It is possible that the type-B void

homogeneous macrostructure. In the figure, black spots in the specimen SM are not voids, but spherical precipitates. Electron probe microanalysis (EPMA) revealed that the spherical precipitates were rich in calcium and poor in titanium. This implies that these precipitates include higher content of perovskite than the matrix, because X-ray diffractometry (Fig. 4) does not indicate the formation of any other additional phase in the as-fabricated specimen SM.

## 2.2 Heat Treatment

Sector specimens of about 1.5 gm were annealed on an alumina dish at 1200 °C to 1500 °C for 30 min in air. The last maximum temperature is nearly equal to the melting point of the hollandite phase.

## 2.3 Measurement

The density of the specimen was measured by the water displacement method. The swelling rate of the specimen was calculated from its density change after heat treatment. The average grain size of perovskite crystals and the characteristics of spherical voids mentioned latter were analyzed by image processing after capture of secondary electron images (SEI) and backscattered electron images (BSI).

## 3. Results

### 3.1 Deformation

The outside views of the specimen SM after the heat treatments at 1500 °C and 1400 °C are shown in Fig. 5. The outer zone of the specimen is partly deformed after heating at 1500 °C, although the specimen retains its shape at 1400 °C. On the other side, the specimen SB entirely got out of shape at 1500 °C. These phenomena might be caused by the melting of hollandite crystals, and softening of hollandite and zirconolite crystals. The summary of data from the specimen SM is presented in Table 2. In the table, the specimen SM shows the swelling rates of about 18 and 25 % at 1500 °C and 1400 °C, respectively. The reason why the rate was larger at the lower temperature is supposed to be due to a thermal stability in microstructures as described in the following section. No remarkable swelling occurred in the specimen below 1300 °C.

### 3.2 Microstructure

A peculiar microstructure was observed in the specimen SM after the heat treatment at 1500 °C. As shown in the microstructure in Fig. 6, fine spherical voids are distributed in the specimen matrix. In the figure, the right-edge zone is of the deformed part named "Falling-down zone (F)". Enlarged images of the voids are indicated in Fig. 7. The feature of the void is divided into the two types, A and B : The type-A void is filled with the separated polyhedral crystals of perovskite, while the type-B void is covered with a film. EPMA reveals that the film was composed of hollandite and zirconolite. It is possible that the type-B void

also contained the separated crystals of perovskite on its film before the specimen was polished for ceramography.

The same feature of spherical voids was also observed in the specimen SM after annealing at 1400 °C. In this case, the average size of the voids was smaller than that in the heat treatment at 1500 °C (Table 2). The macroscopic and enlarged images are shown in Fig. 8, where the macroscopic feature at 1400 °C is quite different from that at 1500 °C (ref. Fig. 6). Some extremely greater voids would escape from the specimen matrix during the heat treatment over 1400 °C.

Further annealing experiments at 1200 °C and 1300 °C were conducted to clarify the nucleation and growth phenomena of the spherical voids. A microstructure after annealing at 1200 °C is shown in Fig. 9. In the figure, micropores are mainly formed within the spherical precipitates. These micropores were not observed in the as-fabricated specimen. This means that annealing at atmospheric pressure facilitates the growth of tiny latent micropores in the precipitates. After the heat treatment at 1300 °C, the micropores grew up to pores of around 1 micrometer, as shown in Fig. 10. This phenomenon is consistent with the fact that a small amount of swelling occurred in the specimen SM (Table 2).

The steep density change between 1300 °C and 1400 °C (Table 2) implies that softening of the specimen matrix may significantly proceed at that temperature. This matrix softening probably accelerates the growth of pores seen in Fig. 10. In that temperature region, the remarkable grain growth of perovskite crystals occurs in both the spherical precipitates (Table 2, Figs. 7 and 8) and the specimen matrix.

### 3.3 Phase

Figure 11 shows X-ray diffraction patterns from the specimen SB before and after the heat treatments at 1500 °C. After this annealing, an additional phase,  $\text{Al}_2\text{TiO}_5$  (designated "A") was formed in the specimen SB. On the other hand, the other additional phase,  $\text{CaAl}_2\text{O}_9$  (designated "X") was formed in the specimen SM, as shown in Fig. 12.

### 3.4 Others

Melting experiments and thermal diffusivity measurements were conducted for the specimens SM and SB, of which the objectives are to get information on thermal properties at high temperature. The results revealed that there was no problem as a fuel matrix on new phase formation up to around 2000 °C, even though an eutectic phase formed at around 1700 °C in the system  $\text{CaO-TiO}_2$ , and that the specimen SM had excellent thermal diffusivity.

## 4. Discussion

### 4.1 Growth Mechanism of Spherical Void

Judging from the results in the specimen SM, the spherical voids are supposed to change their shapes with an increase of the annealing temperature. As illustrated in Fig. 13, the growth process of the spherical voids is supposed to be divided into the four steps from A to D.

also contained the separated crystals of perovskite on its film before the specimen was polished for ceramography.

The same feature of spherical voids was also observed in the specimen SM after annealing at 1400 °C. In this case, the average size of the voids was smaller than that in the heat treatment at 1500 °C (Table 2). The macroscopic and enlarged images are shown in Fig. 8, where the macroscopic feature at 1400 °C is quite different from that at 1500 °C (ref. Fig. 6). Some extremely greater voids would escape from the specimen matrix during the heat treatment over 1400 °C.

Further annealing experiments at 1200 °C and 1300 °C were conducted to clarify the nucleation and growth phenomena of the spherical voids. A microstructure after annealing at 1200 °C is shown in Fig. 9. In the figure, micropores are mainly formed within the spherical precipitates. These micropores were not observed in the as-fabricated specimen. This means that annealing at atmospheric pressure facilitates the growth of tiny latent micropores in the precipitates. After the heat treatment at 1300 °C, the micropores grew up to pores of around 1 micrometer, as shown in Fig. 10. This phenomenon is consistent with the fact that a small amount of swelling occurred in the specimen SM (Table 2).

The steep density change between 1300 °C and 1400 °C (Table 2) implies that softening of the specimen matrix may significantly proceed at that temperature. This matrix softening probably accelerates the growth of pores seen in Fig. 10. In that temperature region, the remarkable grain growth of perovskite crystals occurs in both the spherical precipitates (Table 2, Figs. 7 and 8) and the specimen matrix.

### 3.3 Phase

Figure 11 shows X-ray diffraction patterns from the specimen SB before and after the heat treatments at 1500 °C. After this annealing, an additional phase,  $\text{Al}_2\text{TiO}_5$  (designated "A") was formed in the specimen SB. On the other hand, the other additional phase,  $\text{CaAl}_2\text{O}_9$  (designated "X") was formed in the specimen SM, as shown in Fig. 12.

### 3.4 Others

Melting experiments and thermal diffusivity measurements were conducted for the specimens SM and SB, of which the objectives are to get information on thermal properties at high temperature. The results revealed that there was no problem as a fuel matrix on new phase formation up to around 2000 °C, even though an eutectic phase formed at around 1700 °C in the system  $\text{CaO-TiO}_2$ , and that the specimen SM had excellent thermal diffusivity.

## 4. Discussion

### 4.1 Growth Mechanism of Spherical Void

Judging from the results in the specimen SM, the spherical voids are supposed to change their shapes with an increase of the annealing temperature. As illustrated in Fig. 13, the growth process of the spherical voids is supposed to be divided into the four steps from A to D.

The as-fabricated specimen SM includes the spherical precipitates rich in perovskite. These precipitates contain latent micropores of the remaining gas due to hot pressing at 29 MPa. Since the specimen matrix did not contain such a micropore, void formation was limited only in the precipitates as described above.

In the step A after the heat treatment at 1200 °C, the micropores of less than 1 micrometer in diameter appear in the grain boundaries of perovskite crystals in the spherical precipitates, since a slight softening of the specimen occurs. The formation of micropores is consistent with a slight decrease in density from 4.15 to 4.13 g/cm<sup>3</sup>. In the step B at 1300 °C, the micropores grow up to the pores of around 1 micrometer in diameter due to more softening of the specimen matrix.

In the following step at 1400 °C, on the other hand, softening of the specimen significantly proceeds, and then perovskite crystals are surrounded with expanded pores and separated from each other. In this stage, the spherical precipitates change their features to the spherical voids. In the step D at 1500 °C, the voids grow still more and keep a stable state, where the inner pressure of the voids is assumed to be atmospheric one, because hollandite in the matrix is in the melting condition and sufficient matrix softening occurs.

#### 4.2 Formation Mechanism of New Phases

The new phases A and X were formed in the specimen SB and SM, respectively, after the heat treatment only at 1500 °C. The deformed outer zone of the specimen SM included a large amount of the new phase X, while the inner part (block) contained a small amount of X (Fig. 12). Any additional phase did not occur in annealing at 1400 °C. The formation processes of these new phases are well explained by the schematic mechanism presented in Fig. 14.

##### (1) Al<sub>2</sub>TiO<sub>5</sub> Phase ("A") in Specimen SB

Hollandite is assumed to be decomposed to the phase A, BaO and TiO<sub>2</sub> during the heat treatment at 1500 °C that is nearly equal to the melting point of the original phase. When the annealed specimen is quenched, these decomposition products would be detected (Case 2 in Fig. 14). Although in slow cooling, almost all of the decomposition products would recombine to hollandite (Case 1 in Fig. 14). In the case 2, the peak intensity of hollandite lines in a X-ray diffraction pattern would decrease owing to the formation of the phase A. Decrease in relative intensity of hollandite peaks in Fig. 11 supports the present mechanism. Among the decomposition products, BaO may be trapped again in the barium site of another hollandite crystal, since X-ray diffractometry did not detect that phase.

##### (2) CaAl<sub>12</sub>O<sub>19</sub> Phase ("X") in Specimen SM

In the deformed outer zone of the specimen SM, the spherical voids escaped and perovskite agglomerates would be formed since the voids included many perovskite crystals (Fig. 7). During the heat treatment at 1500 °C, hollandite may be also decomposed to the phase A, BaO and TiO<sub>2</sub>. The phase A would react with perovskite agglomerates and form the phase X (Case 3 in Fig. 14). This phase would be easily detected after quenching of the specimen. As the inner part of the specimen retained its shape, the voids were still present, which prevented the

agglomeration of perovskite crystals. Consequently, the limited reaction between perovskite and the phase A would form only a small amount of the phase X (Fig. 12).

## 5. Conclusion

Thermal durability of the two kinds of Synroc specimens was examined to develop a new type reactor fuel named "Waste Disposal Possible (WDP) Fuel". The fuel has two functions of a reactor fuel and waste form. The phase composition of the modified Synroc specimen, designated "SM", was changed to improve the thermal durability of the reference Synroc specimen, designated "SB". These specimens were subjected to the heat treatments at 1200 °C to 1500 °C.

After annealing of sector specimens at 1400 °C and 1500 °C for 30 min in air, spherical voids were observed in the specimen SM that basically retained its shape, while no voids were detected in the specimen SB that was completely deformed. Average sizes of the voids in the specimen SM were 41 and 28 micrometers at 1500 °C and 1400 °C, respectively. The voids are assumed to be filled with polyhedral perovskite crystals of which the average sizes were about 10 and 5 micrometers at 1500 °C and 1400 °C, respectively. The formation of voids in the specimen SM caused the swelling of 18 and 25 % at 1500 °C and 1400 °C, respectively. No detectable deformations in the two kinds of Synroc specimens were observed below 1300 °C.

Further annealing experiments at 1200 °C and 1300 °C revealed that the as-fabricated specimen SM had already included latent micropores in the spherical precipitates rich in perovskite. These latent micropores would increase their sizes when the specimen was softened. Conclusively, it was supposed that the formation of the spherical voids resulted from the existence of the spherical precipitates in the as-fabricated specimen SM.

New phases of  $\text{Al}_2\text{TiO}_5$  (Phase A) and  $\text{CaAl}_2\text{O}_9$  (Phase X) were formed in the specimens SB and SM, respectively, after the heat treatment only at 1500 °C. The phase A is one of the decomposition products of hollandite, and the phase X comes from the reaction between the phase A and perovskite. The deformed outer zone of the specimen SM was richer in the phase X than the inner matrix which retained its original shape. Softening and degasification, caused the deformation of the outer zone of the specimen SM, may possibly make perovskite agglomerates and facilitate the reaction described above.

A homogeneous microstructure is inevitable for the prevention of void formation in the specimen SM at high temperature, since the precipitates rich in perovskite contained latent tiny micropores that caused specimen swelling. However, homogeneous microstructure and degasification of an as-fabricated specimen may be achieved by the improvement of preparation process. For instance, a conventional sintering process will make it easy to degas a specimen. By the way, as presented in Appendix 2, the modified Synroc material has relatively superior thermal properties, which is the very important fact and gives us an encouragement to continue the present investigation. Although the modified Synroc material is one of promising candidates for WDP fuel, many other characteristics need to be examined prior to practical utilization in future.

agglomeration of perovskite crystals. Consequently, the limited reaction between perovskite and the phase A would form only a small amount of the phase X (Fig. 12).

## 5. Conclusion

Thermal durability of the two kinds of Synroc specimens was examined to develop a new type reactor fuel named "Waste Disposal Possible (WDP) Fuel". The fuel has two functions of a reactor fuel and waste form. The phase composition of the modified Synroc specimen, designated "SM", was changed to improve the thermal durability of the reference Synroc specimen, designated "SB". These specimens were subjected to the heat treatments at 1200 °C to 1500 °C.

After annealing of sector specimens at 1400 °C and 1500 °C for 30 min in air, spherical voids were observed in the specimen SM that basically retained its shape, while no voids were detected in the specimen SB that was completely deformed. Average sizes of the voids in the specimen SM were 41 and 28 micrometers at 1500 °C and 1400 °C, respectively. The voids are assumed to be filled with polyhedral perovskite crystals of which the average sizes were about 10 and 5 micrometers at 1500 °C and 1400 °C, respectively. The formation of voids in the specimen SM caused the swelling of 18 and 25 % at 1500 °C and 1400 °C, respectively. No detectable deformations in the two kinds of Synroc specimens were observed below 1300 °C.

Further annealing experiments at 1200 °C and 1300 °C revealed that the as-fabricated specimen SM had already included latent micropores in the spherical precipitates rich in perovskite. These latent micropores would increase their sizes when the specimen was softened. Conclusively, it was supposed that the formation of the spherical voids resulted from the existence of the spherical precipitates in the as-fabricated specimen SM.

New phases of  $\text{Al}_2\text{TiO}_5$  (Phase A) and  $\text{CaAl}_2\text{O}_9$  (Phase X) were formed in the specimens SB and SM, respectively, after the heat treatment only at 1500 °C. The phase A is one of the decomposition products of hollandite, and the phase X comes from the reaction between the phase A and perovskite. The deformed outer zone of the specimen SM was richer in the phase X than the inner matrix which retained its original shape. Softening and degasification, caused the deformation of the outer zone of the specimen SM, may possibly make perovskite agglomerates and facilitate the reaction described above.

A homogeneous microstructure is inevitable for the prevention of void formation in the specimen SM at high temperature, since the precipitates rich in perovskite contained latent tiny micropores that caused specimen swelling. However, homogeneous microstructure and degasification of an as-fabricated specimen may be achieved by the improvement of preparation process. For instance, a conventional sintering process will make it easy to degas a specimen. By the way, as presented in Appendix 2, the modified Synroc material has relatively superior thermal properties, which is the very important fact and gives us an encouragement to continue the present investigation. Although the modified Synroc material is one of promising candidates for WDP fuel, many other characteristics need to be examined prior to practical utilization in future.



## Acknowledgement

The authors would like to express their thanks to Mr.K.Ishimoto, Director of the Department of Hot Laboratories, for his kindly support to the activity of the present working group, and also to Mr.T.Yamahara, General Manager of Hot Engineering Division in the department, for his useful comments.

## References

- 1) A.E.Ringwood et al., "Immobilization of High Level Nuclear Reactor Waste in Synroc", *Nature* 278 (1979)
- 2) W.J.Buykx et al., "Titanium Ceramics for the Immobilization of Sodium-Bearing High Level Nuclear Waste", *J.Am.Ceram.Soc.*, 71 (8) (1988)
- 3) K.D.Reeve et al., "Radioactive Waste Forms for the Future--- Chat. 4 SYNROC", Elsevier Science Publishers B.V., 1988
- 4) K.L.Smith et al., "Structural Features of Zirconolite, Hollandite and Perovskite, the Major Waste-Bearing Phases in Synroc", *Geoscience Applications* (1993)
- 5) E.R.Vance et al., "High Temperature Study of  $\text{CaZrTi}_2\text{O}_7$ ", *J.Nucl.Mater.*, 190 (1992)
- 6) R.B.Roberts et al., "Thermal Expansion of Zirconolite", *J.Nucl.Mater.*, 148 (1987)

## APPENDIX Additional Information and Thermal Properties

### Appendix 1 Crystal Structures and Phases of Synroc Minerals

Crystal structures of Synroc minerals (perovskite, hollandite and zirconolite) are indicated in Fig. A-1. The fundamental unit in the structures is  $\text{TiO}_6$  octahedron. Perovskite has a tetragonal structure comprising of the octahedrons and locates calcium atom at the body center position. In the cases of hollandite and zirconolite, the structures consist of the combination of octahedral twins or octahedral pairs. As clearly seen in these structures, the atoms Ca, Ba and Zr are surrounded with a octahedral chain. In a Synroc waste forms, these atoms are replaced with FPs and TRUs.

Phase diagrams of the minerals are summarized in Fig. A-2. These minerals are sufficiently stable up to their melting points, if their compositions do not change. Perovskite has the highest melting point (around  $2000^\circ\text{C}$ ), while hollandite and zirconolite have low values (around  $1500^\circ\text{C}$ ). In these minerals, non-stoichiometric regions exist near their melting points. On the other hand, the two eutectic phases exist in both sides of the perovskite composition in the system  $\text{CaO}-\text{TiO}_2$  (Fig. A-3).

## Acknowledgement

The authors would like to express their thanks to Mr.K.Ishimoto, Director of the Department of Hot Laboratories, for his kindly support to the activity of the present working group, and also to Mr.T.Yamahara, General Manager of Hot Engineering Division in the department, for his useful comments.

## References

- 1) A.E.Ringwood et al., "Immobilization of High Level Nuclear Reactor Waste in Synroc", *Nature* 278 (1979)
- 2) W.J.Buykx et al., "Titanium Ceramics for the Immobilization of Sodium-Bearing High Level Nuclear Waste", *J.Am.Ceram.Soc.*, 71 (8) (1988)
- 3) K.D.Reeve et al., "Radioactive Waste Forms for the Future--- Chat. 4 SYNROC", Elsevier Science Publishers B.V., 1988
- 4) K.L.Smith et al., "Structural Features of Zirconolite, Hollandite and Perovskite, the Major Waste-Bearing Phases in Synroc", *Geoscience Applications* (1993)
- 5) E.R.Vance et al., "High Temperature Study of  $\text{CaZrTi}_2\text{O}_7$ ", *J.Nucl.Mater.*, 190 (1992)
- 6) R.B.Roberts et al., "Thermal Expansion of Zirconolite", *J.Nucl.Mater.*, 148 (1987)

## APPENDIX Additional Information and Thermal Properties

### Appendix 1 Crystal Structures and Phases of Synroc Minerals

Crystal structures of Synroc minerals (perovskite, hollandite and zirconolite) are indicated in Fig. A-1. The fundamental unit in the structures is  $\text{TiO}_6$  octahedron. Perovskite has a tetragonal structure comprising of the octahedrons and locates calcium atom at the body center position. In the cases of hollandite and zirconolite, the structures consist of the combination of octahedral twins or octahedral pairs. As clearly seen in these structures, the atoms Ca, Ba and Zr are surrounded with a octahedral chain. In a Synroc waste forms, these atoms are replaced with FPs and TRUs.

Phase diagrams of the minerals are summarized in Fig. A-2. These minerals are sufficiently stable up to their melting points, if their compositions do not change. Perovskite has the highest melting point (around  $2000^\circ\text{C}$ ), while hollandite and zirconolite have low values (around  $1500^\circ\text{C}$ ). In these minerals, non-stoichiometric regions exist near their melting points. On the other hand, the two eutectic phases exist in both sides of the perovskite composition in the system  $\text{CaO}-\text{TiO}_2$  (Fig. A-3).

## Acknowledgement

The authors would like to express their thanks to Mr.K.Ishimoto, Director of the Department of Hot Laboratories, for his kindly support to the activity of the present working group, and also to Mr.T.Yamahara, General Manager of Hot Engineering Division in the department, for his useful comments.

## References

- 1) A.E.Ringwood et al., "Immobilization of High Level Nuclear Reactor Waste in Synroc", *Nature* 278 (1979)
- 2) W.J.Buykx et al., "Titanium Ceramics for the Immobilization of Sodium-Bearing High Level Nuclear Waste", *J.Am.Ceram.Soc.*, 71 (8) (1988)
- 3) K.D.Reeve et al., "Radioactive Waste Forms for the Future --- Chat. 4 SYNROC", Elsevier Science Publishers B.V., 1988
- 4) K.L.Smith et al., "Structural Features of Zirconolite, Hollandite and Perovskite, the Major Waste-Bearing Phases in Synroc", *Geoscience Applications* (1993)
- 5) E.R.Vance et al., "High Temperature Study of  $\text{CaZrTi}_2\text{O}_7$ ", *J.Nucl.Mater.*, 190 (1992)
- 6) R.B.Roberts et al., "Thermal Expansion of Zirconolite", *J.Nucl.Mater.*, 148 (1987)

## APPENDIX Additional Information and Thermal Properties

### Appendix 1 Crystal Structures and Phases of Synroc Minerals

Crystal structures of Synroc minerals (perovskite, hollandite and zirconolite) are indicated in Fig. A-1. The fundamental unit in the structures is  $\text{TiO}_6$  octahedron. Perovskite has a tetragonal structure comprising of the octahedrons and locates calcium atom at the body center position. In the cases of hollandite and zirconolite, the structures consist of the combination of octahedral twins or octahedral pairs. As clearly seen in these structures, the atoms Ca, Ba and Zr are surrounded with a octahedral chain. In a Synroc waste forms, these atoms are replaced with FPs and TRUs.

Phase diagrams of the minerals are summarized in Fig. A-2. These minerals are sufficiently stable up to their melting points, if their compositions do not change. Perovskite has the highest melting point (around  $2000^\circ\text{C}$ ), while hollandite and zirconolite have low values (around  $1500^\circ\text{C}$ ). In these minerals, non-stoichiometric regions exist near their melting points. On the other hand, the two eutectic phases exist in both sides of the perovskite composition in the system  $\text{CaO}-\text{TiO}_2$  (Fig. A-3).

## Appendix 2 Melting Experiments and Thermal Diffusivity Measurements

### (1) Melting Experiments and Results

Using the specimens SM and SB, melting experiments have been carried out at about 1200 °C to 2000 °C, of which the objectives are to detect thermal arrests and to examine the formation of additional new phases in heating and cooling processes.

A fine granular sample set in a crucible of tungsten was heated up to around 2000 °C at a constant heating rate in a high vacuum, and followed to cooling at the same rate after kept it at the maximum temperature for about 5 min (the specimen SM). The temperature at the bottom of the crucible was precisely measured by an infrared ray thermometer.

The temperature changes in the specimens SM and SB are indicated in Fig. A-4. A cyclic change seen in the specimen SB might come from the variation of thermal capacity occurred in the system, since a part of sample evaporated from the crucible at about 1600 °C and above around 1800 °C during the experiment. The species evaporated, as shown in Fig. A-5, are composed of Synroc minerals and an undefined new-phase, designated "X". In the specimen SM after heating, on the other side, no evaporation did not occur and any new-phase formation was not observed. The difference in the evaporation phenomena between the specimens SM and SB implies that the specimen SM has an excellent thermal durability above around 1500 °C.

As indicated in both specimens (Fig. A-4), the first thermal arrests appear at about 1400 °C to around 1500 °C. These arrests would result from the melting of hollandite and zirconolite and also the formation of an eutectic phase rich in TiO<sub>2</sub> (see Fig. A-3). Only in the specimen SM, however, the second thermal arrest can be seen at around 1700 °C, which is assumed due to the formation of another eutectic phase rich in CaO with the eutectic temperature of 1740 °C (Fig. A-3). This eutectic phase is stable only at this temperature, so that it can not be detected in the specimen after cooling.

### (2) Thermal Diffusivity Measurements and Results

Thermal diffusivities of the specimens SM and SB were measured at RT to 1100 °C with an interval of about 200 °C. A measuring procedure is presented in Fig. A-6. The experimental specimens were the disk of about 3 mm in diameter and around 1 mm in length.

The data of thermal diffusivities for both specimens are shown in Fig. A-7. The diffusivity of the specimen SM is greater than that of SB by factors of about 40 % and about 10 % in lower and higher temperature regions, respectively. Such an excellent thermal diffusivity of the specimen SM might come from the high content of perovskite in the specimen, because perovskite has superior thermal diffusivity in Synroc minerals.

**Table 1 Measured Densities and Calculated Phase Compositions of Specimens SM and SB**

Specimen	Density (g/cc)	Element Content (w/o)			
		Perovskite	Hollandite	Zirconolite	Rutile
Modif. Synroc SM	4.152	60	30	10	-
Ref. Synroc SB	4.230	20	30	30	20

**Table 2 Data Summary for Heat Treatment Experiments in Specimen SM**

Heat Treatment Temperature C	Density g/cc	Swelling v/o	Perovskite Grain Size $\mu$ m	Spherical Void	
				Av. Size $\mu$ m	Occu. Rate %
1500	3.53	18	10	41	23
1400	3.31	25	5	28	34
1300	4.05	2	1	----	----
1200	4.13	----	1>	----	----
Before Heating	4.15	--	1>	--	--

\* Occu. Rate.....Rate of area occupied with voids

\* Heating time : 30 min.      \* Atmosphere : Air-1 atm condition

\* Density.....Immersion method

\* Swelling...Calculated by density change ( No weight change )

\* Spherical void : Obtained by image analyses

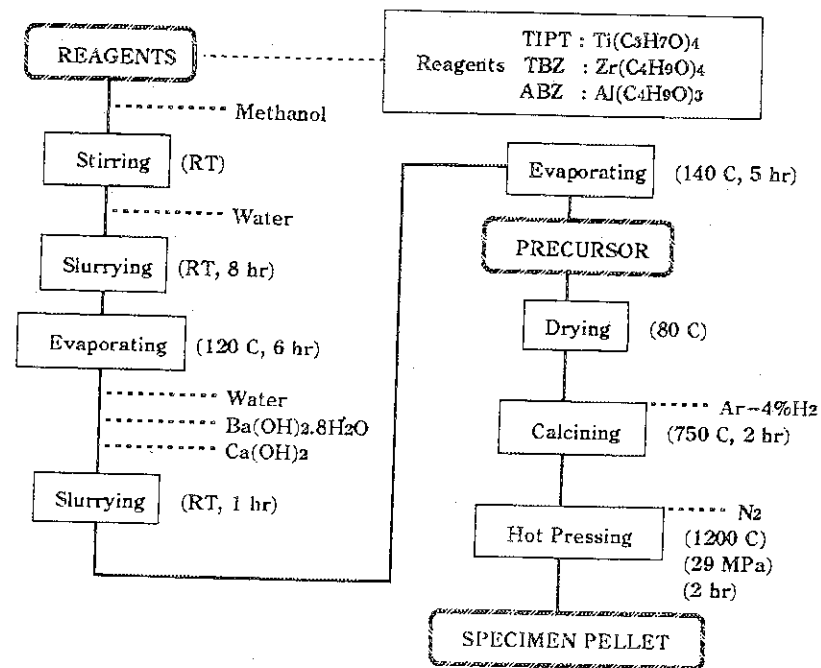


Fig. 1 Preparation Process of Specimens

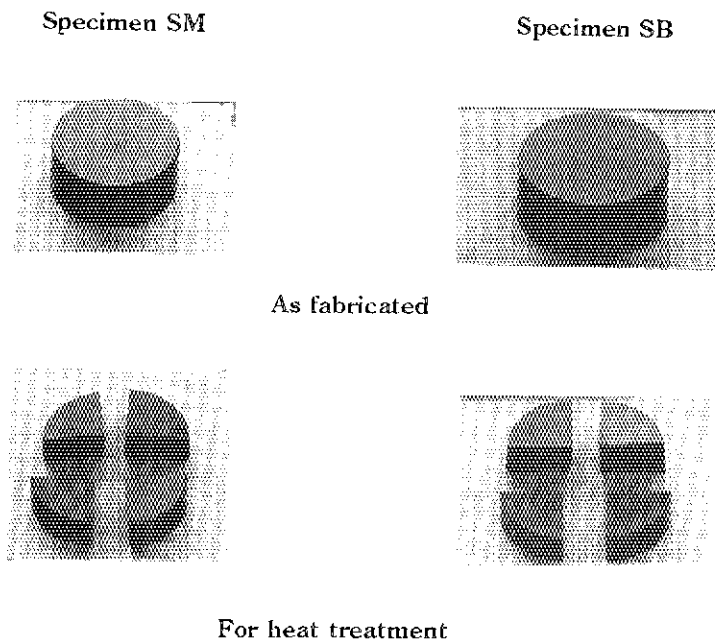


Fig. 2 Outside Views of As-Fabricated Specimens SM and SB

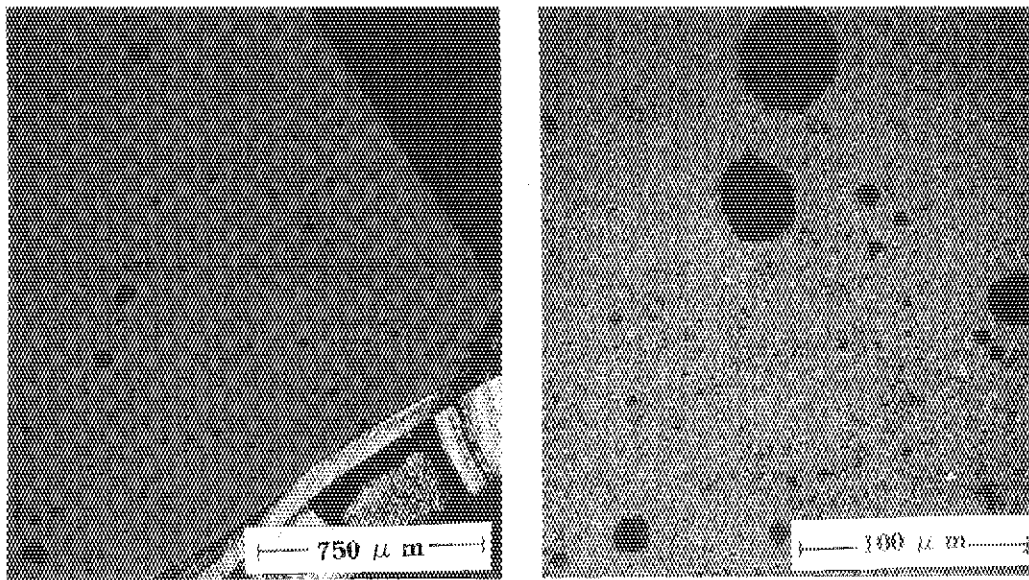


Fig. 3 Spherical Precipitates in As-Fabricated Specimen SM

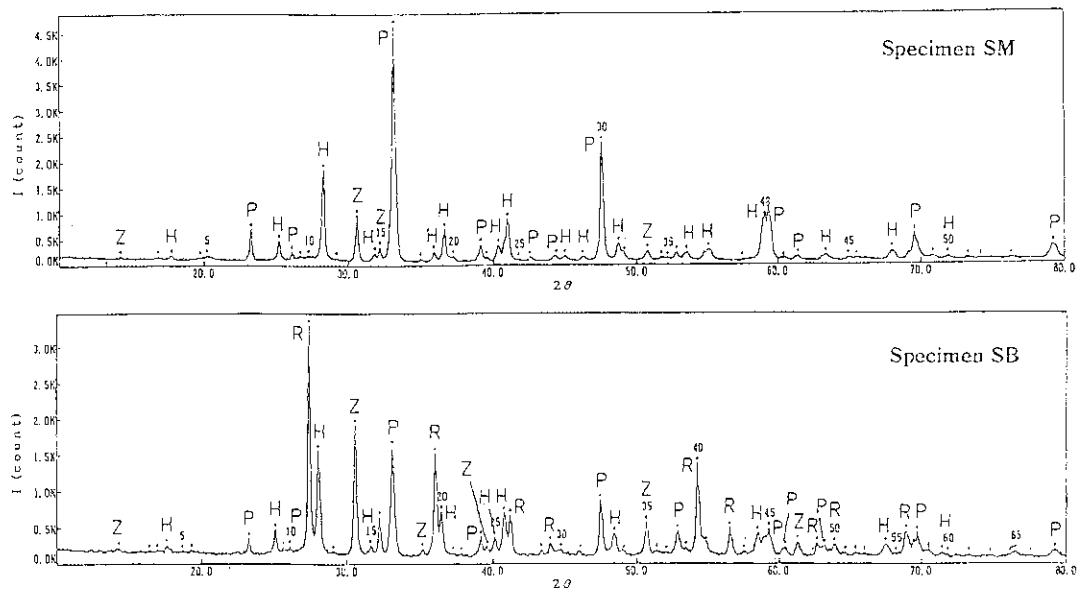


Fig. 4 X Ray Powder Diffraction Patterns from Specimens SM and SB

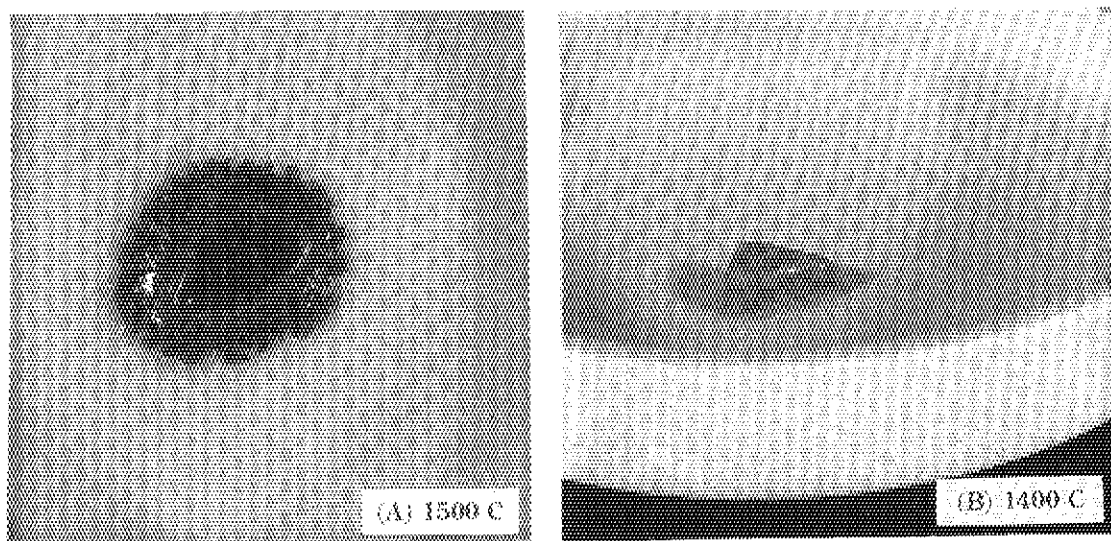


Fig. 5 Outside Views of Specimen SM after Heat Treatments at 1500 C (A) and 1400 C (B)

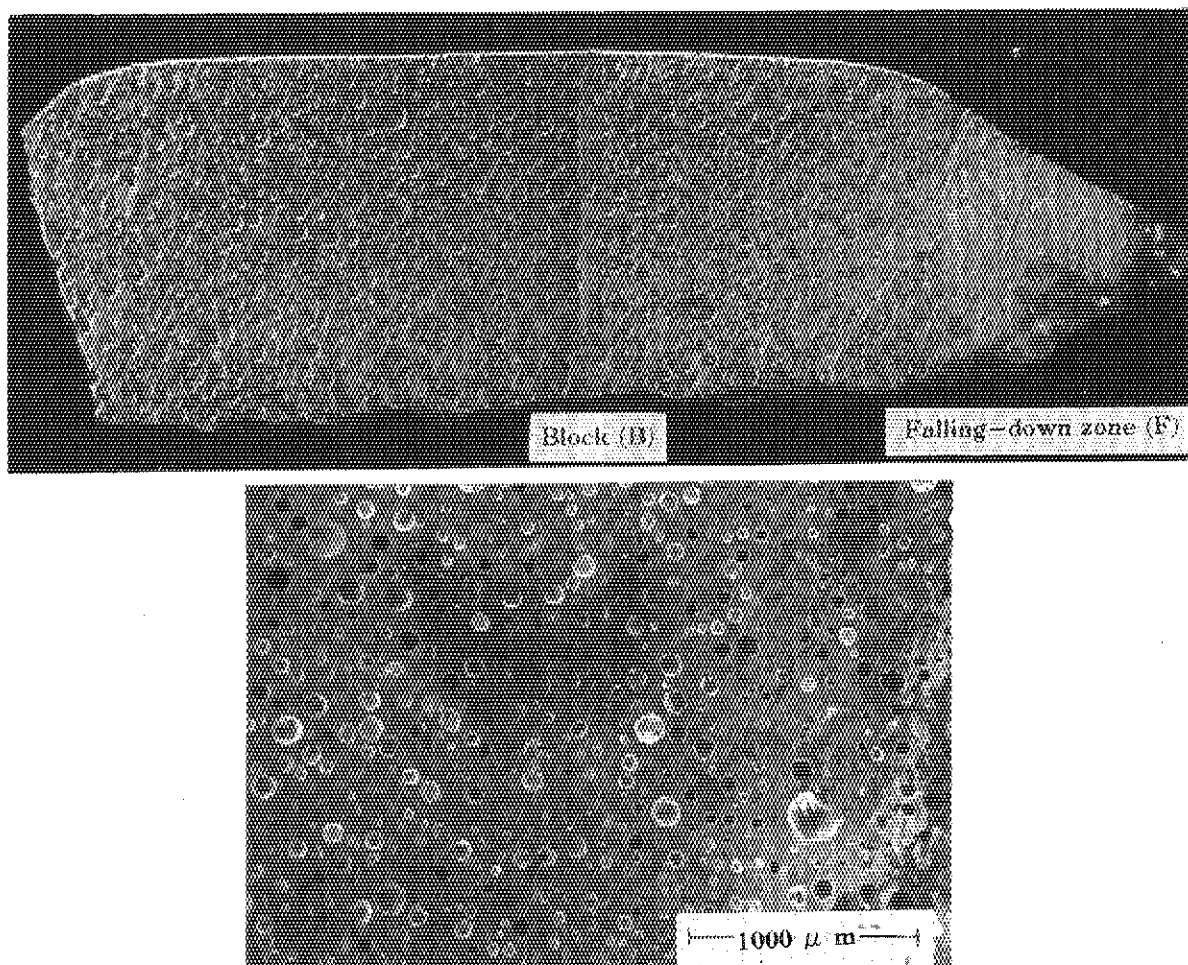


Fig. 6 Macroscopic Feature and Spherical Voids in Specimen SM after Heat Treatment at 1500 C



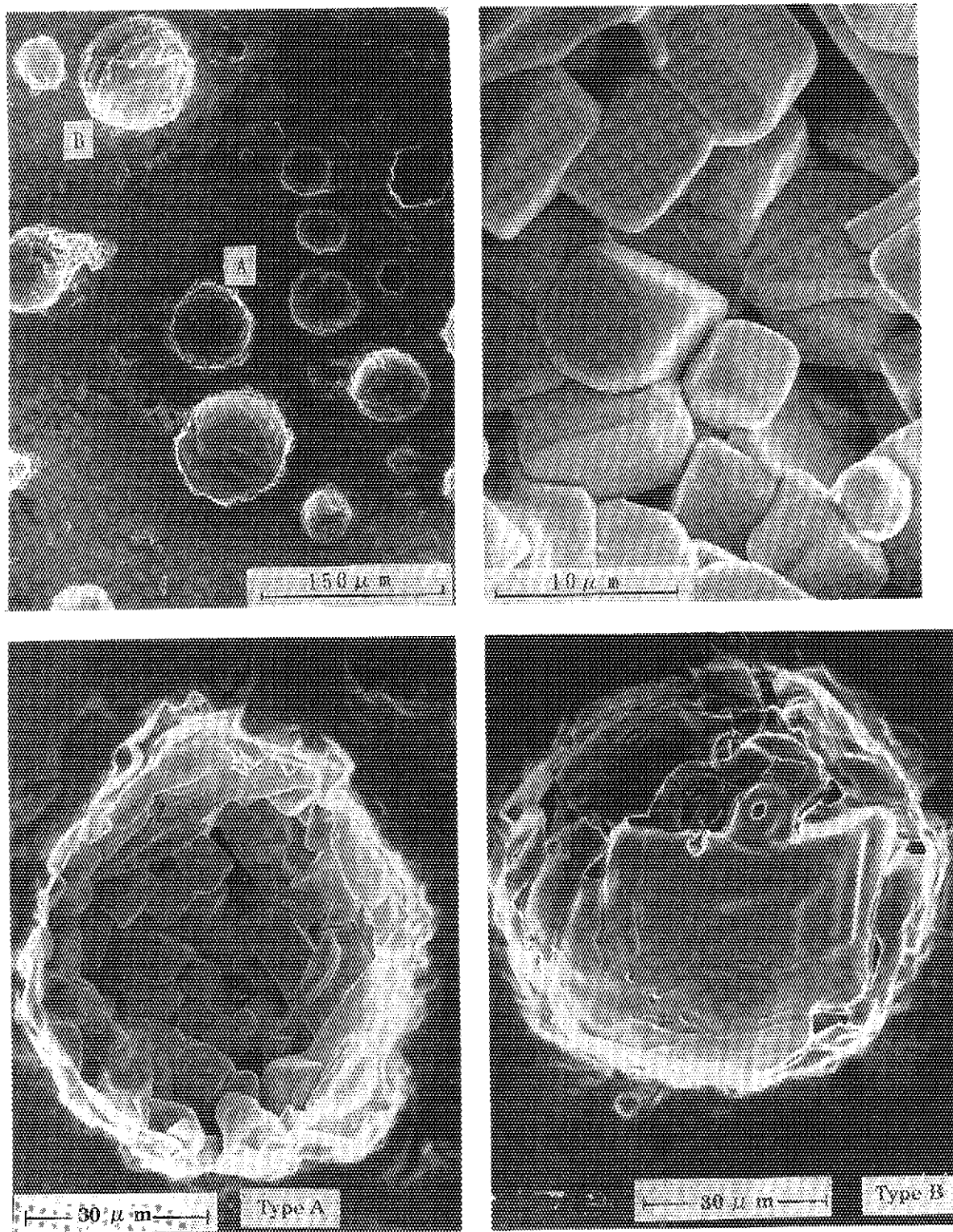


Fig. 7 Enlarged Feature of Two Types of Spherical Voids A and B

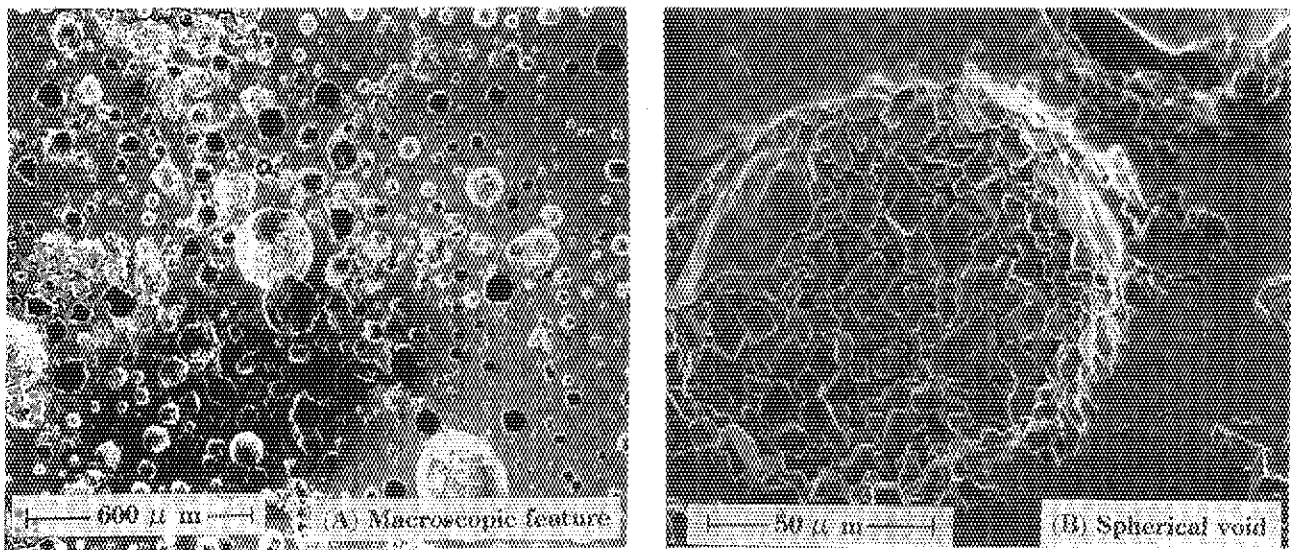


Fig. 8 Macroscopic Feature (A) and Spherical Void (B) in Specimen SM after Heat Treatment at 1400 C

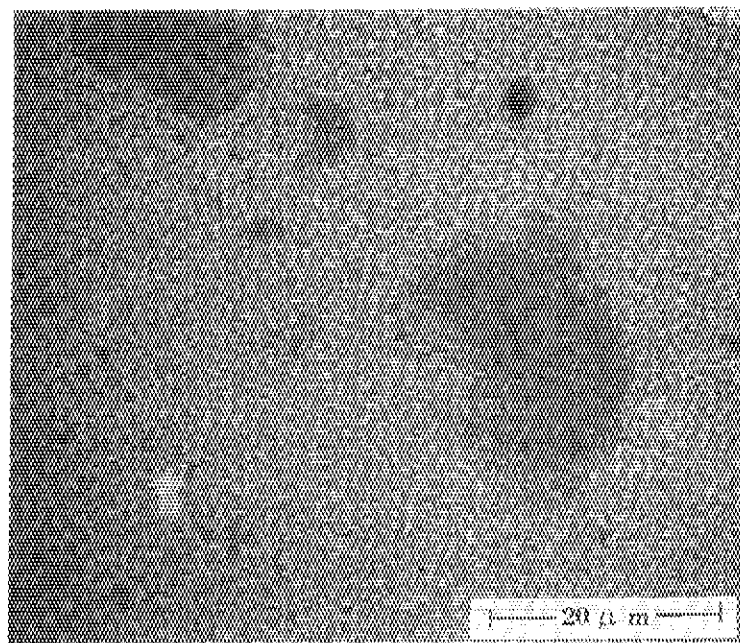


Fig. 9 Micropores in Spherical Precipitates of Specimen SM after Heat Treatment at 1200 C



Fig. 10 Pores in Specimen SM after Heat Treatment at 1300 C

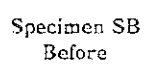


Fig. 11 X Ray Powder Diffraction Patterns from Specimen SB  
before and after Heat Treatments at 1500 C  
(F...Falling - Down Zone)

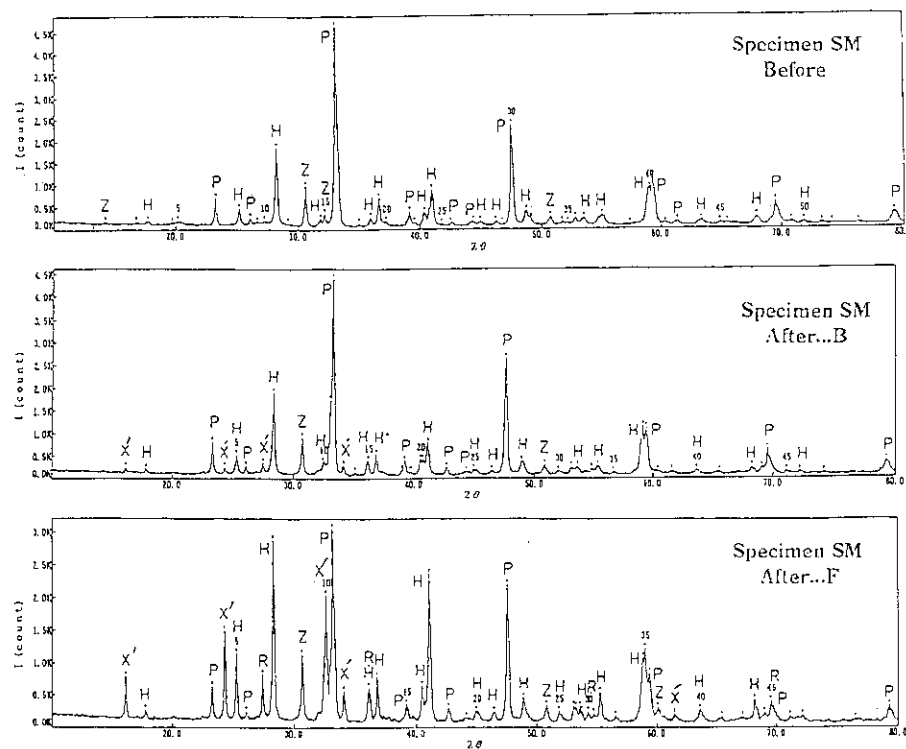


Fig. 12 X Ray Powder Diffraction Patterns from Specimen SM  
before and after Heat Treatments at 1500 C  
(B....Block Zone ; F....Falling-Down Zone)

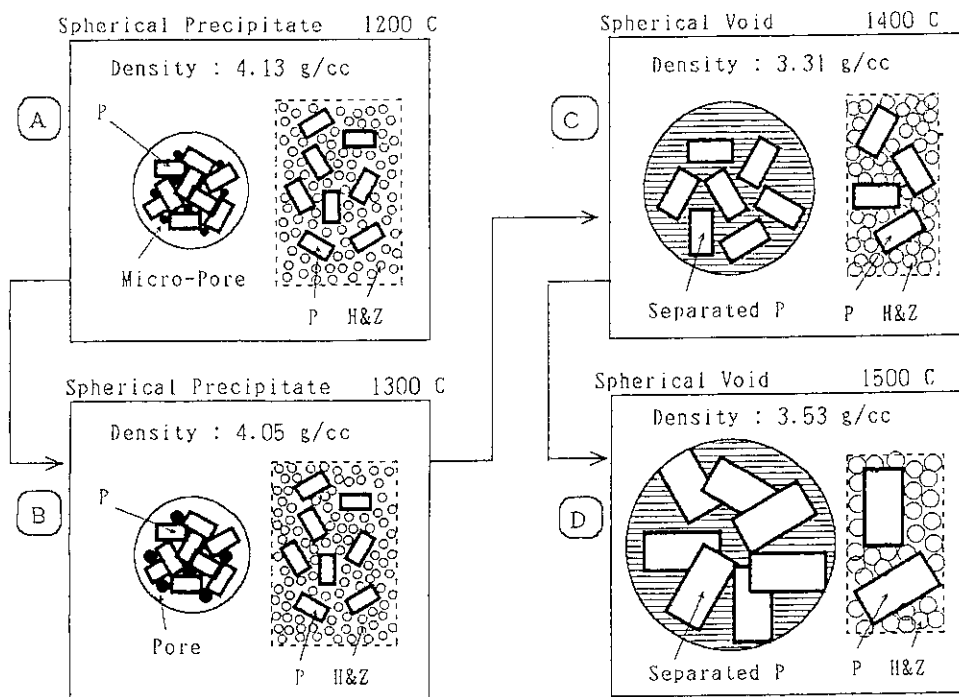


Fig. 13 Growth Process of Spherical Precipitate to Spherical Void  
(Left....Precipitate or Void ; Right....Matrix)

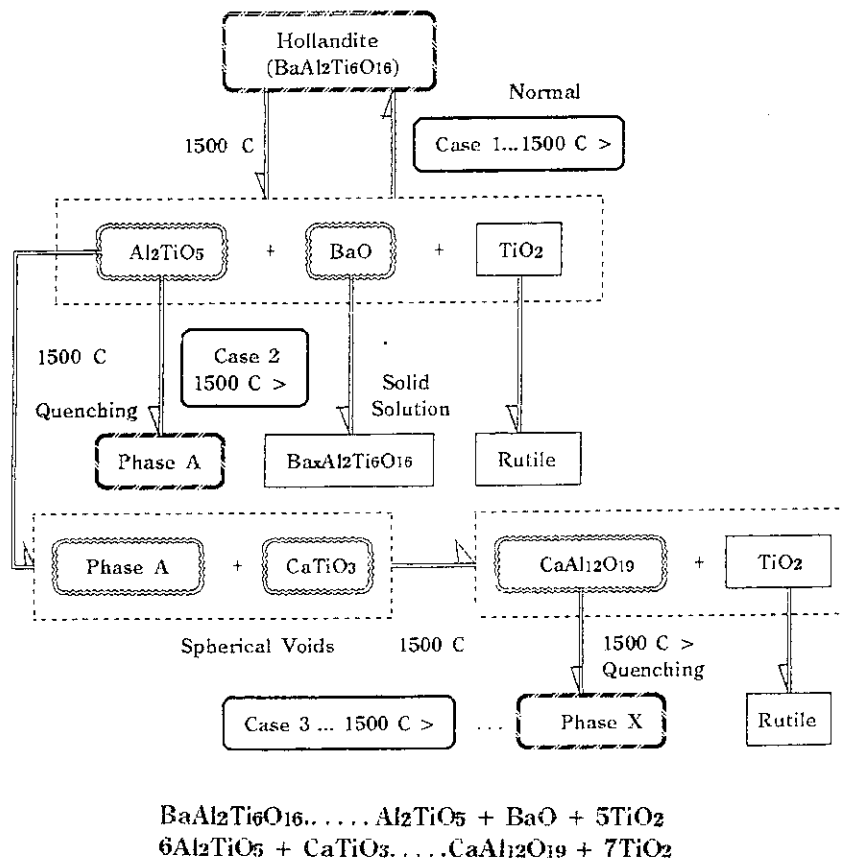


Fig. 14 Formation Process of Phase A and Phase X

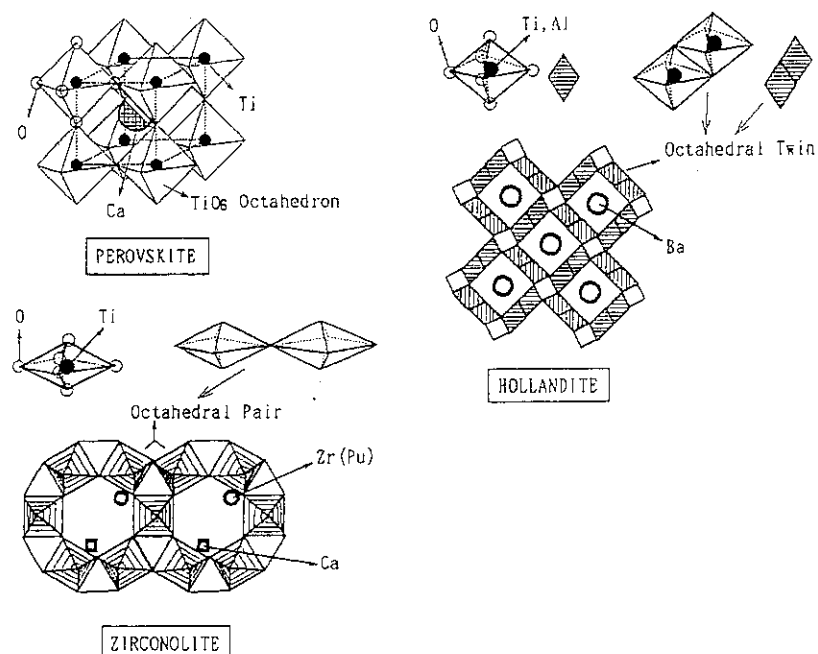


Fig. A-1 Crystal Structures of Perovskite, Hollandite and Zirconolite

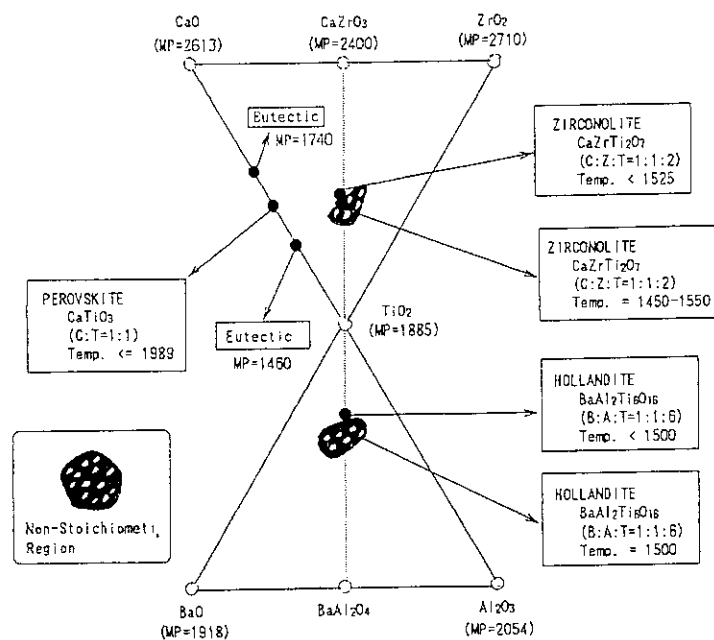
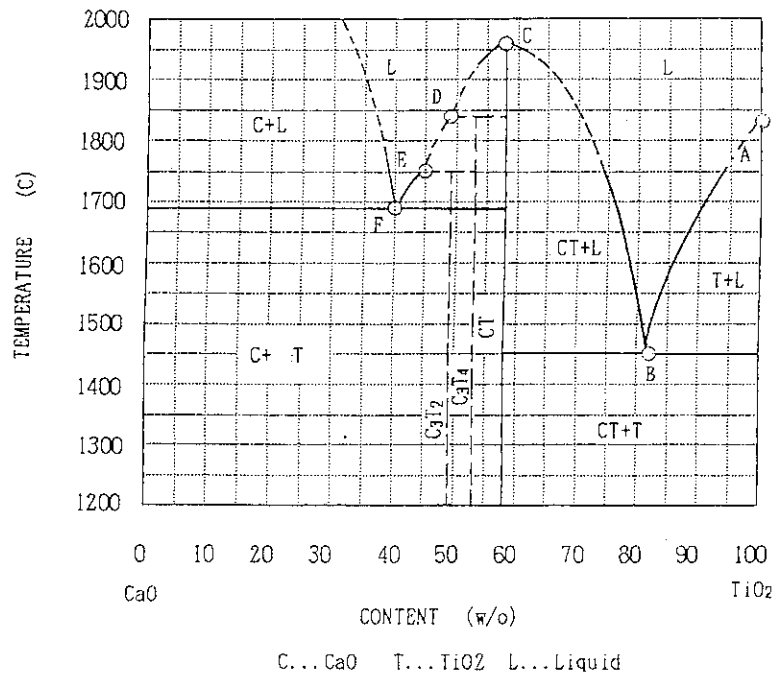
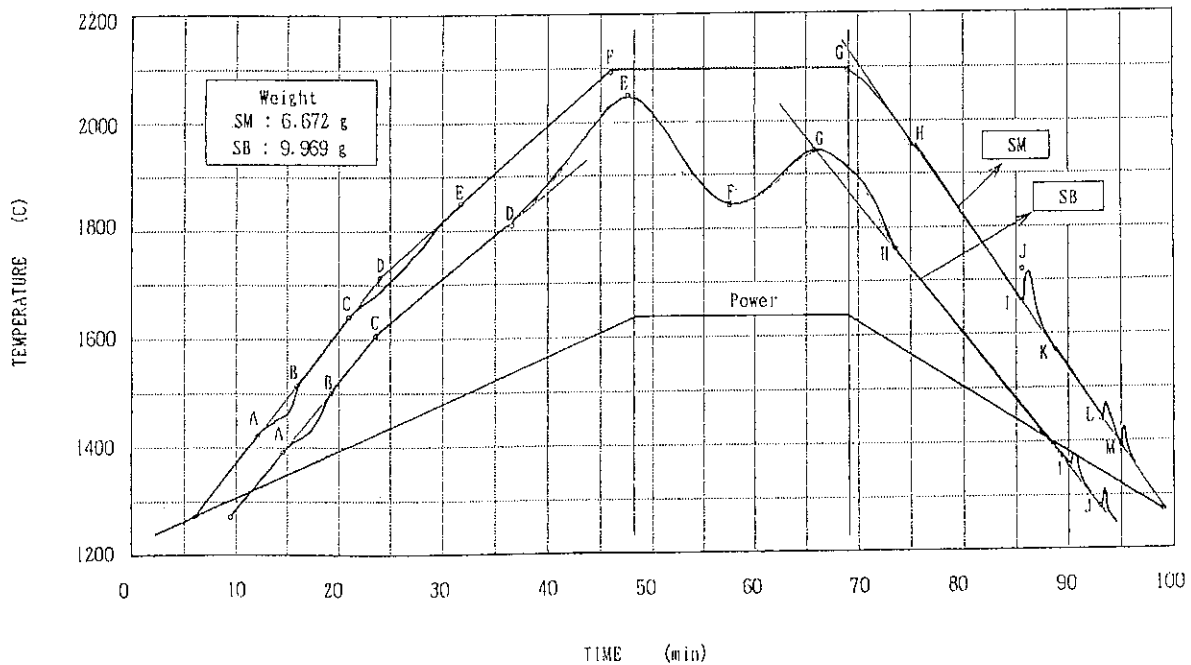


Fig. A-2 Phase Diagrams in Perovskite, Hollandite and Zirconolite

Fig. A-3 Phase Diagram in System CaO-TiO<sub>2</sub>

TEMPERATURE

SM : A=1420 B=1515 C=1637 D=1713 E=1848 F=2092 G=2002 H=1951 I=1656 J=1710 K=1566 L=1439 M=1389

SB : A=1389 B=1502 C=1605 D=1810 E=2027 F=1835 G=1944 H=1759 I=1349 J=1272

Fig. A-4 Thermal Arrests in High Temperature Region of Specimens SM and SB  
(Melting Experiments)

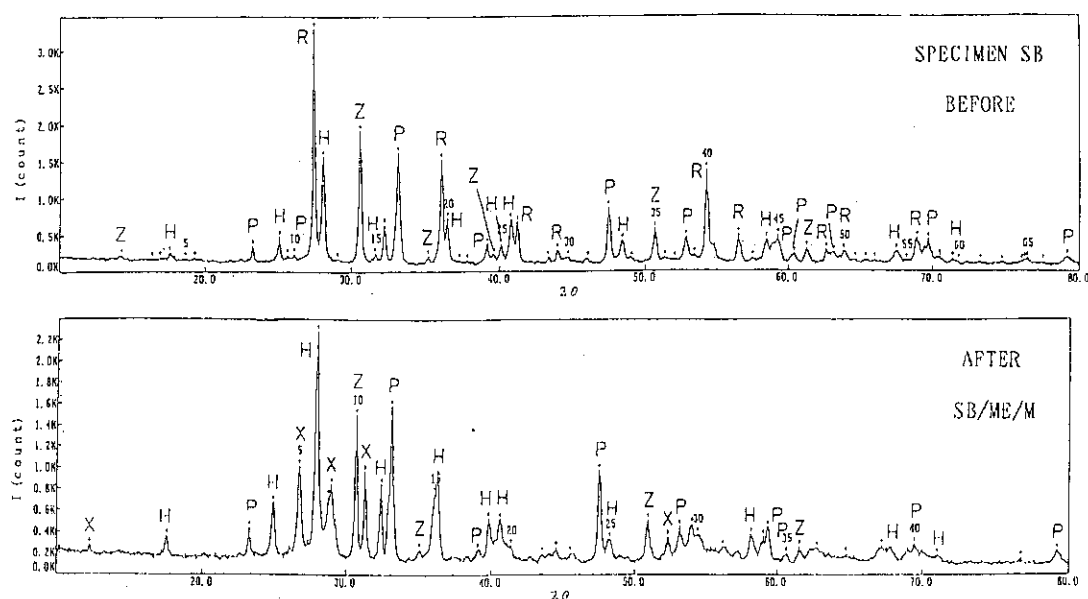


Fig. A-5 X Ray Powder Diffraction Patterns from Specimen SB after Melting Experiment

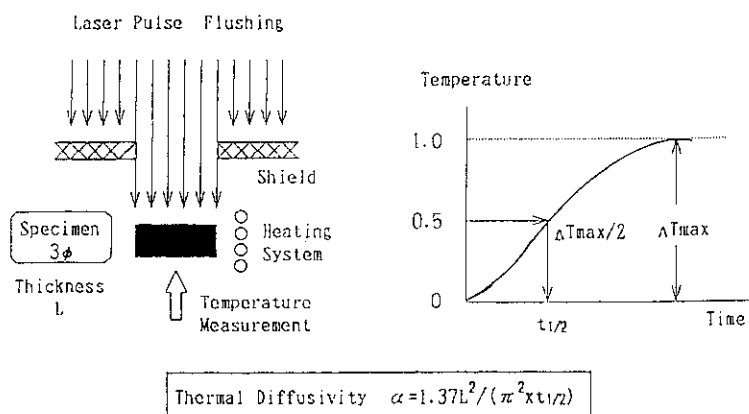


Fig. A-6 Experimental Procedure in Thermal Diffusivity Measurement



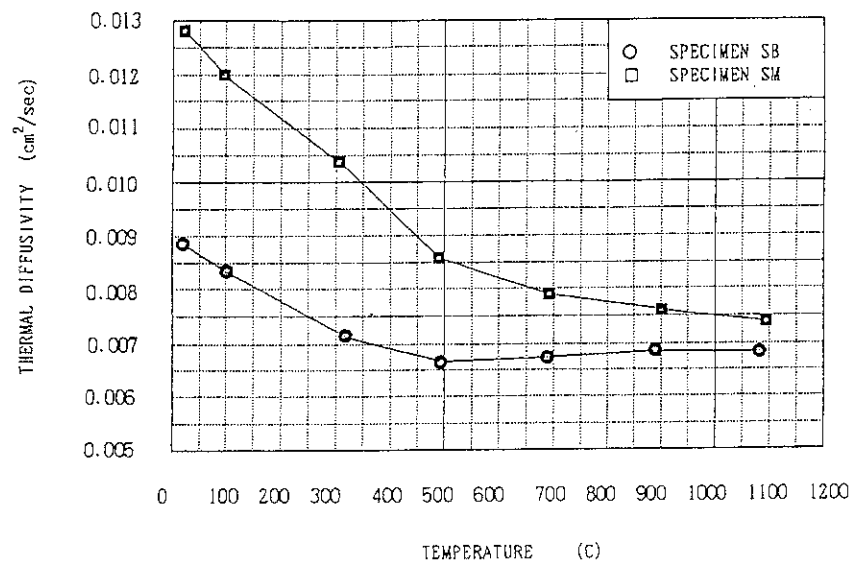


Fig. A-7 Thermal Diffusivities of Specimens SM and SB